American Mineralogist, Volume 62, pages 623–633, 1977

Iron-titanium oxides of the Dufek intrusion, Antarctica

GLEN R. HIMMELBERG

U.S. Geological Survey and Department of Geology
University of Missouri, Columbia, Missouri 65201

AND A. B. FORD

U.S. Geological Survey, Menlo Park, California 94025

Abstract

The Dufek intrusion is a stratiform mafic body 8 to 9 km thick underlying 24,000 to 34,000 km² in the Pensacola Mountains, Antarctica. Textures, structures, magmatic stratigraphy, and chemical variation indicate that layered gabbros and related rocks of this body developed by crystal accumulation on a magma chamber floor. Major cumulus phases in the exposed part of the intrusion are plagioclase, Ca-rich pyroxene, Ca-poor pyroxene, and iron–titanium oxide minerals. Modal amounts of cumulus oxide minerals, ferrian ilmenite and titaniferous magnetite, generally range from 2 to 12 percent.

Existing textures and compositions of the oxide minerals largely reflect subsolidus recrystallization and equilibration. Nevertheless, the amounts of vanadium and aluminum in ilmeno-magnetite are reliable indicators of fractionation trends in the magma during crystallization of the oxide minerals. Application of experimental T–$f(O_2)$–X relations suggests that, for most of the intrusion with cumulus iron–titanium oxide minerals, conditions of crystallization and cooling were close to the conditions of the quartz–fayalite–magnetite buffer essentially parallel to ilmenite isopleths. An oxygen fugacity of $10^{-10.1}$ bar is inferred for primary crystallization at 1090°C.

Introduction

The Dufek intrusion is a stratiform body of mafic rock that makes up nearly the entire northern third of the Pensacola Mountains (Fig. 1). Structure, rock textures, and the relation of whole rock and cumulus mineral chemistry to magmatic stratigraphy indicate that the rocks developed by accumulation of crystals on the floor of a magma chamber. This study is a part of a continuing, detailed investigation of the mineralogy of the rock units and the chemical variation of individual mineral phases, in order better to understand the conditions of differentiation and cooling of the complex. In this report we are specifically concerned with the distribution, chemical variations, fractionation trends, and conditions of primary crystallization and subsolidus recrystallization of the cumulus oxide minerals. (Following the usage of Buddington and Lindsley, 1964, the term 'oxide minerals' as used in this paper refers to opaque minerals in the system FeO–Fe_2O_3–TiO_2). Preliminary results of this study were reported in an earlier article (Himmelberg and Ford, 1975).

General features of the Dufek intrusion

The geologic setting and major features of the Dufek intrusion have been discussed in detail by Ford and Boyd (1968), Ford (1970, 1976), and Himmelberg and Ford (1976), and only a brief summary of those features relevant to this study is given here. The layered cumulates are exposed in two partial, non-overlapping stratigraphic sections (Fig. 1). The lowermost 1.8 km of exposed rocks make up the Dufek Massif section. The upper exposed section, the Forrestal Range section, is approximately 1.7 km thick and contains at its top a 300 m thick concordant layer of granophyre. The total thickness is not directly known because two parts of the body, the basal section and an intermediate section between the two ranges, are not exposed. The intermediate section is estimated to be 2–3 km thick (Ford, 1976), and geophysical evidence suggests that the basal section is 1.8–3.5 km thick (Behrendt *et al.*, 1974, p. 14). Thus the total thickness of layered rocks may be as much as 8–9 km. Geophysical reconnaissance surveys (Behrendt *et al.*, 1974) indicate that the body underlies a

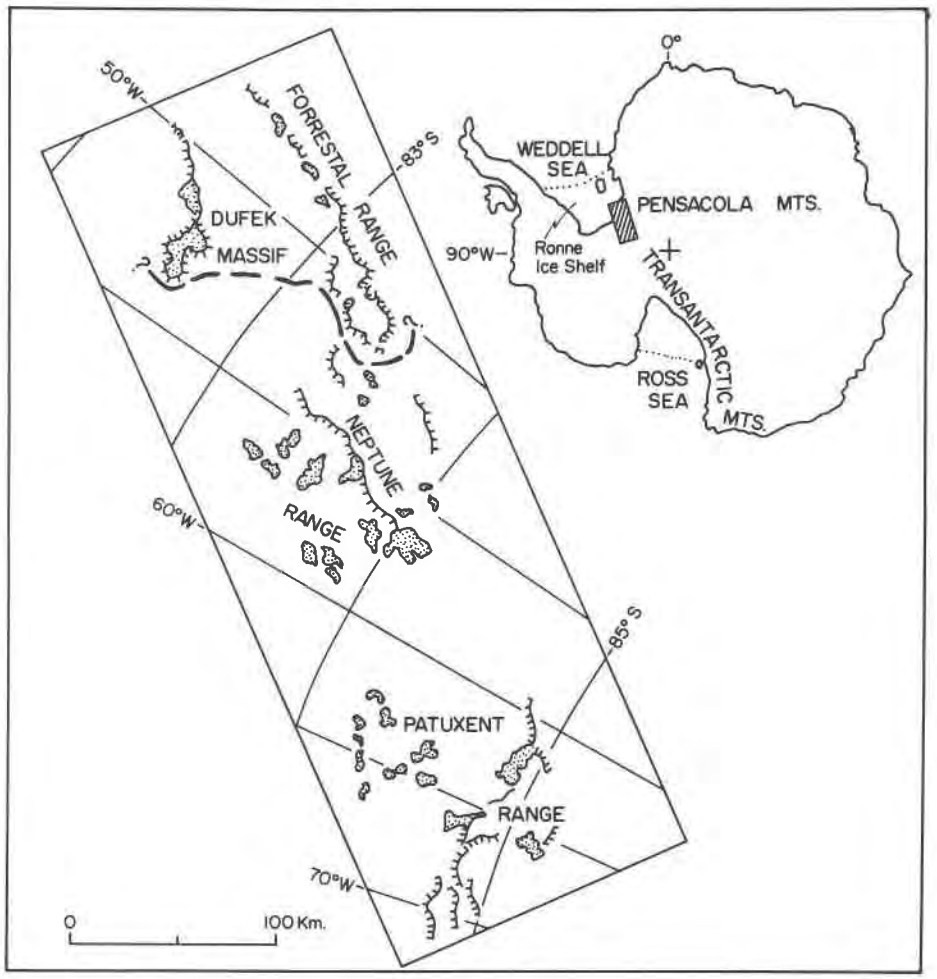

Fig. 1. Index map showing extent of the Dufek intrusion in the Pensacola Mountains. Heavy dashed line marks contact of gabbro on north with Permian and other sedimentary rocks to the south. Stippled areas show major outcrops. Crests of major rock and ice escarpments are shown by hachured lines.

region of at least 24,000 to 34,000 km²; hence it is one of the world's largest known stratiform complexes.

Distribution of cumulus phases is shown in Figure 2 relative to a generalized columnar section and principal rock stratigraphic units. The columnar section is a composite of 21 measured sections. Plagioclase, calcium-rich pyroxene, calcium-poor pyroxene, and oxide minerals are the major cumulus phases. The dominant rock type is plagioclase–pyroxene cumulate, with cumulus oxide minerals abundant in the Forrestal Range section. Layers of plagioclase cumulate are less abundant. Some thin layers that consist of virtually a single cumulus phase grade upward into cumulates of gabbroic composition.

The rocks show an overall enrichment in iron relative to magnesium upward through the sequence (Ford, 1970). Amounts of total iron, titanium, vanadium, and oxide minerals increase upward through the layered sequence. Calcium-poor pyroxenes in the series bronzite-inverted pigeonite range upward from $Ca_{3.5}Mg_{69.1}Fe_{27.4}$ to $Ca_{11.4}Mg_{34.0}Fe_{54.6}$. Calcium-rich pyroxenes in the series augite–ferroaugite trend upward from $Ca_{36.4}Mg_{48.7}Fe_{14.9}$ to $Ca_{30.0}Mg_{23.5}Fe_{46.5}$ (Himmelberg and Ford, 1976).

Distribution and petrography of the oxide minerals

Oxide minerals first occur as cumulus phases approximately 200 m from the top of the Dufek Massif section (Fig. 2). Except in layers of plagioclase cumulate, cumulus oxide minerals continue upward through the gabbro of the Forrestal Range section. Proportions of cumulus oxide minerals typically range from 2 percent to 8–12 percent by volume (Table 1), with some thin layers of nearly 100 percent

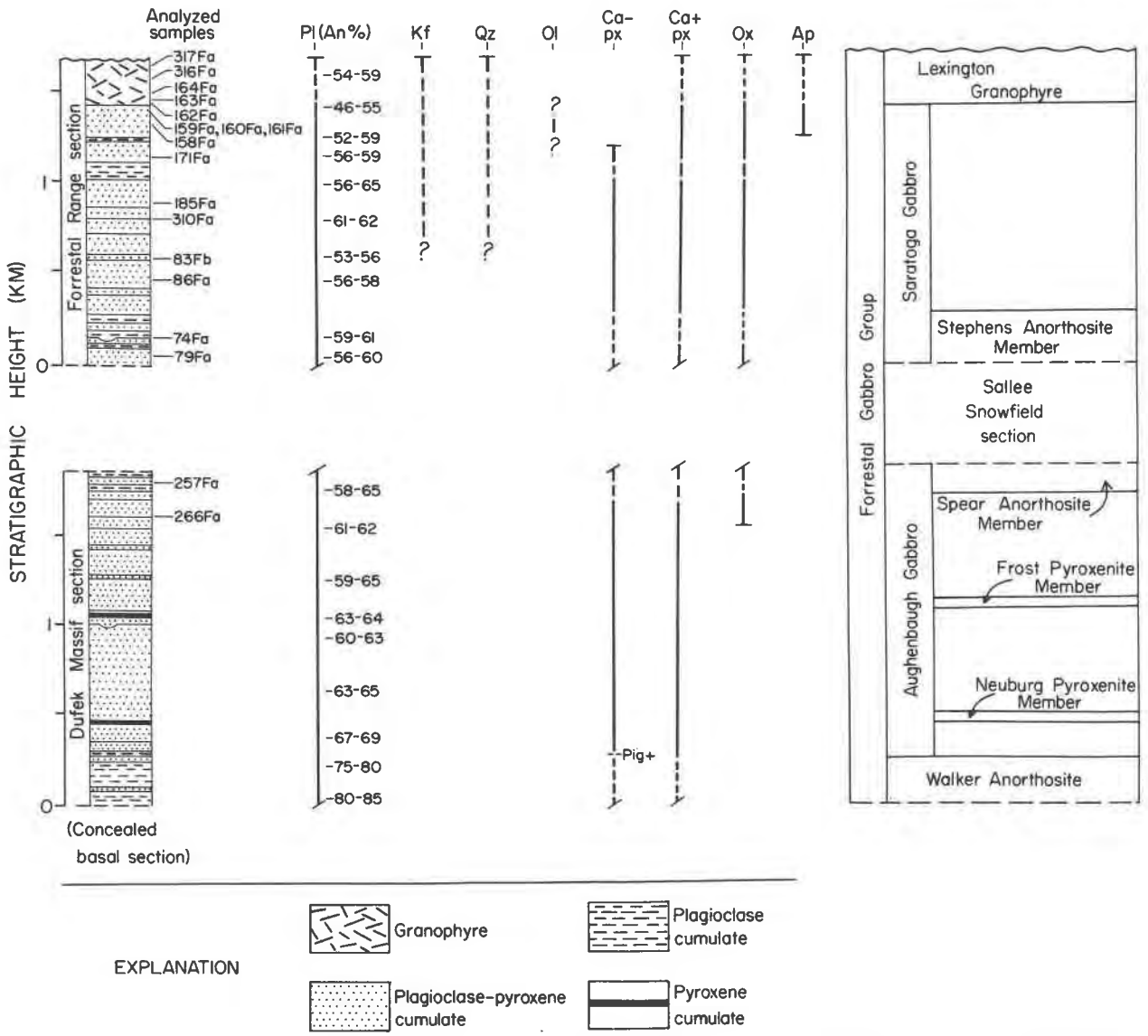

Fig. 2. Generalized composite columnar section and major rock-stratigraphic units of the Dufek intrusion, showing sampled locations. Stratigraphic distribution of cumulus minerals shown by solid lines; postcumulus minerals and, in granophyre, noncumulus minerals shown by broken lines. Pig$^+$ denotes the lowest occurrence of cumulus inverted pigeonite. Pl, plagioclase; Kf, potassium feldspar; Qz, quartz; Ol, olivine; Ca$^-$px, calcium-poor pyroxene; Ca$^+$px, calcium-rich pyroxene; Ox, iron–titanium oxides; Ap, apatite. From Himmelberg and Ford (1976). Rock-stratigraphic nomenclature from Ford (1976).

oxide minerals. Oxide minerals are also ubiquitous minor constituents in the noncumulate granophyre layer. Below the first occurrence of cumulus oxide minerals and in the plagioclase cumulate layers, oxide minerals occur as rare postcumulus grains.

The terminology used to describe the oxide minerals follows the usage of Buddington and others (1963) and Anderson (1968):

Titaniferous magnetite: an optically homogeneous Fe–Ti spinel phase having an oxide stoichiometry approximately R_3O_4.

Ferrian ilmenite: an optically homogeneous Fe–Ti rhombohedral phase having an oxide stoichiometry of about R_2O_3 with Fe_2O_3 less than 50 mole percent.

Ilmeno-magnetite: A regular intergrowth of ferrian ilmenite lamellae in a titaniferous magnetite host.

The oxide minerals generally occur as a titaniferous magnetite host with ferrian ilmenite lamellae

Table 1. Locations and petrographic data for analyzed samples

Sample No.	Height[1]	Location[2]	Lithology[3]	Total oxide minerals[4]
317Fa	1631	FR, Mt. Zirzow	Granophyre	1.4
316Fa	1564	do.	do.	1.7
164Fa	1457	FR, Sorna Bluff	do.	3.1
163Fa	1426	do.	do.	3.7
162Fa	1402	do.	do.	4.8
161Fa	1366	do.	Pl-fag-ox-ap cumulate	4.8
160Fa	1347	do.	do.	8.5
159Fa	1338	do.	do.	11.5
158Fa	1317	do.	do.	12.9
171Fa	1088	do.	Pl-pig-ag-ox cumulate	7.3
185Fa	863	do.	do.	4.5
310Fa	753	do.	do.	7.8
83Fb	525	FR, Mt. Stephens	Pl-pig-fag-ox cumulate	8.4
86Fa	424	do.	do.	7.5
74Fa	114	do.	do.	3.3
79Fa	20	do.	Pl-pig-ag-ox cumulate	6.2
257Fa	1814	DM, Spear Spur	do.	2.1
266Fa	1609	do.	do.	4.4

[1] *Heights are stratigraphic heights in meters measured or estimated above the base of each composite section.*

[2] *FR, Forrestal Range; DM, Dufek Massif. Localities are of type or reference sections given in Ford (1976).*

[3] *Cumulus minerals indicated in order of decreasing abundance: pl, plagioclase; ag, augite; fag, ferroaugite; pig, pigeonite (now inverted to orthopyroxene); ox, oxide minerals; ap, apatite.*

[4] *Volume percent; determined by point counting of large rock slabs and (or) thin sections.*

parallel to {111} (ilmeno-magnetite), intergrown with a coarse, irregular, optically homogeneous ferrian ilmenite to form a composite ilmeno-magnetite–ferrian ilmenite grain (Fig. 3). The amounts, size, and spacing of ferrian ilmenite lamellae in titaniferous magnetite host vary from sample to sample. Ferrian ilmenite also occurs as discrete grains dispersed amongst the silicates, but such grains are not abundant and were not observed in all samples. Exsolution lamellae were not observed within the ferrian ilmenite.

Buddington and Lindsley (1964) proposed that increasing degrees of oxidation and diffusion result in a systematic series of oxide mineral textures ranging from a single-phase, homogeneous titaniferous magnetite, through ferrian ilmenite lamellae in a titaniferous magnetite host, to composite grains of ferrian ilmenite and titaniferous magnetite that formed by granule 'exsolution.' Consistent with the above proposal we interpret the textures of the Dufek oxide minerals to reflect different generations of titaniferous magnetite and ferrian ilmenite, as follows:

Stage I: magmatic crystallization of a homogeneous titaniferous magnetite and, for those samples with discrete ilmenite grains, a coexisting ferrian ilmenite.

Stage II: subsolidus granule 'exsolution' of the primary titaniferous magnetite to form composite grains of titaniferous magnetite (of lower ulvospinel content than the primary grains) and ferrian ilmenite.

Stage III: subsolidus 'exsolution' of Stage II titaniferous magnetite forming ferrian ilmenite lamellae in a titaniferous magnetite host. Diffusion rates, and hence in most cases temperature, would be greater for Stage II than for Stage III (Buddington and Lindsley, 1964). No titaniferous magnetite of Stage I or Stage II is preserved, but ferrian ilmenite of all three stages is present.

Chemistry of the oxide minerals

Analytical procedures

Oxide minerals from 18 samples containing previously analyzed pyroxenes (Himmelberg and Ford, 1976) were analyzed with an ARL EMX-SM electron

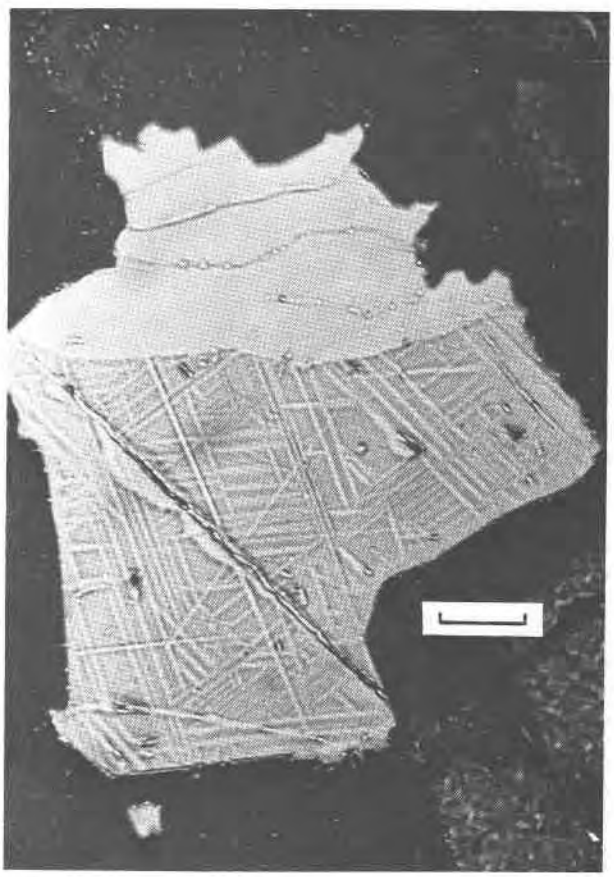

Fig. 3. Representative texture of cumulus iron–titanium oxide minerals in the Dufek intrusion. Ilmeno-magnetite, consisting of ferrian ilmenite lamellae parallel to {111} in a titaniferous magnetite host, forms a composite grain with coarse, irregular ferrian ilmenite. Length of scale bar is 0.1 mm. Sample 74Fa.

microprobe. Natural ferrian ilmenite, titaniferous magnetite, and chromite of known composition were used as standards. Corrections were made for background, mass absorption, secondary fluorescence, and atomic number. Iron was determined as total iron, and the amounts of Fe_2O_3 and FeO were calculated from stoichiometric considerations using the procedures outlined by Carmichael (1967). Carmichael's method was also used to calculate the proportion of $TiFe_2O_4$ in titaniferous magnetite and of R_2O_3 in ferrian ilmenite.

An electron beam of approximately 1 μm diameter was used to analyze titaniferous magnetite host and ferrian ilmenite. Ilmeno-magnetite was analyzed by step traversing with a beam of 25 μm diameter to obtain an approximate bulk composition of the host titaniferous magnetite plus ilmenite lamellae. Analyses of those samples for which the most complete data were obtained relative to determining the conditions of formation are presented in Tables 2 through 4. Analyses of titaniferous magnetite host and ferrian ilmenite of composite grains for other samples are available upon request.

Titaniferous magnetite host

For each sample, analyses were made at five to seven points on each of two or three grains. Points within a single grain commonly show a range in composition of 10 to 15 and in some cases as much as 25 mole percent $TiFe_2O_4$. The largest ranges in composition are associated with samples having abundant fine ferrian ilmenite lamellae difficult to resolve optically. Thus the apparent inhomogeneity may be in part a result of analyzing two unmixed phases rather than a single spinel phase, and any definitive statement of homogeneity of the titaniferous magnetite host is precluded. The range in composition for all samples is approximately from 5 to 50 mole percent $TiFe_2O_4$.

In Table 2, analyses of titaniferous magnetite host are given for three samples in which ferrian ilmenite lamellae were also analyzed. Those analyses identified by a superscript on the sample number are for points adjacent to (within 2 μm) the ferrian ilmenite lamella with the same superscript. Analyses of titaniferous magnetite more removed from ferrian ilmenite lamellae have no superscript on the sample number. Although no systematic study of zoning across boundaries between titaniferous magnetite and ferrian ilmenite lamellae was made, points adjacent to ilmenite lamellae show a depletion in titanium and an increase in iron relative to the more general titaniferous magnetite host compositions (Table 2, Sample 74Fa). Mathison (1975) demonstrated a similar pattern in the titaniferous magnetite host from the Somerset Dam layered intrusion, Australia.

Ferrian ilmenite

Individual ferrian ilmenite grains and lamellae are chemically homogeneous, and the proportion of R_2O_3 for all samples ranges from 0.1 to 5.8 mole percent.

Mathison (1975), in his study of the Somerset Dam intrusion, documented consistent compositional differences between discrete ferrian ilmenite grains, which he called primary ilmenite, and ilmenite lamellae and intergrowths with titaniferous magnetite, which he termed secondary ilmenite. In almost all cases the secondary ferrian ilmenite contained less R_2O_3 than the primary grains from the same sample. In the Dufek intrusion, discrete grains of ferrian ilmenite are not abundant, but in the two samples where comparisons were made (74Fa and 171Fa, Table 3 and 4) there are no significant differences in R_2O_3 between discrete grains and coarse intergrowths with ilmeno-magnetite. On the other hand, some ferrian ilmenite lamellae do have less R_2O_3 than the coarse composite grains (Tables 2 and 3). In addition different ferrian ilmenite lamellae, even within the same host grain, may have different R_2O_3 contents.

For sample 74Fa the manganese content is successively greater in discrete ferrian ilmenite, ferrian ilmenite of composite grains, and ferrian ilmenite lamellae in titaniferous magnetite host (Tables 2 through 4). Sample 171Fa shows no significant difference in manganese content between discrete and composite ferrian ilmenite grains, but the manganese content is greater in the ferrian ilmenite lamellae. Similar distribution of manganese has been reported by Neumann (1974) and Mathison (1975). Lindsley (1976, written communication) demonstrated that the increasing manganese values are consistent with the experimentally-determined distribution of MnO between magnetite and ilmenite with decreasing temperature. In general, when compared to titaniferous magnetite host, ferrian ilmenite contains more manganese and less aluminum, vanadium, and chromium.

Ilmeno-magnetitite

Bulk analyses of titaniferous magnetite host plus ferrian ilmenite lamellae are given in Table 3. Each tabulated analysis is an average of 2 or 3 grains. The difference in amounts of individual oxides between

Table 2. Analyses of host titaniferous magnetite and ferrian ilmenite lamellae of the Dufek intrusion

Magnetite	74Fa	74Fa[1]	74Fa[2]	74Fa[3]	171Fa	164Fa[1]	164Fa[2]	164Fa[3]	164Fa[4]	164Fa[5]
SiO_2	0.56	0.56	0.56	0.56	0.45	0.61	0.57	0.65	0.66	0.71
TiO_2	5.42	1.06	1.61	1.61	10.3	9.42	7.39	10.8	11.3	9.44
Al_2O_3	2.17	1.26	2.17	2.17	1.87	0.85	0.95	0.67	1.09	0.15
Cr_2O_3	0.64	0.47	0.52	0.53	0.06	0.02	0.02	--	0.01	0.02
*Fe_2O_3	52.8	63.4	61.9	59.3	46.7	49.3	53.3	47.0	46.1	50.0
FeO	35.9	32.5	33.4	34.4	40.9	40.7	38.9	42.1	42.8	40.8
MnO	0.27	0.09	0.20	0.20	0.28	0.42	0.30	0.40	0.45	0.43
MgO	0.20	0.06	0.03	0.09	0.34	--	--	--	0.02	0.01
CaO	0.11	0.11	0.11	0.11	0.23	0.06	0.06	0.05	0.05	0.04
Total	98.1	99.6	100.5	100.2	101.1	101.3	101.5	101.7	102.5	101.6
Mole % Ulvospinel	17.8	5.2	6.7	10.3	30.5	28.1	22.9	32.7	33.7	29.2

Ilmenite	74Fa[1]	74Fa[2]	74Fa[3]	74Fa[4]	74Fa[5]	171Fa[1]	171Fa[2]	171Fa[3]	164Fa[1]	164Fa[2]	164Fa[3]	164Fa[4]	164Fa[5]
SiO_2	0.58	0.58	0.58	0.58	0.58	0.52	0.57	0.75	0.58	0.55	0.59	0.59	0.69
TiO_2	49.5	49.5	49.0	50.8	50.3	52.3	50.9	51.6	50.4	50.2	49.8	50.1	50.8
Al_2O_3	0.43	0.48	0.33	0.12	0.07	0.05	0.18	0.03	0.13	0.20	0.06	0.08	0.07
Cr_2O_3	0.47	0.24	0.10	0.10	0.08	--	0.04	--	--	--	--	--	--
*Fe_2O_3	4.86	5.20	4.36	3.01	3.50	0.73	2.06	1.62	4.11	3.65	4.26	3.77	3.06
FeO	42.6	42.3	42.7	43.5	43.2	46.3	45.2	45.7	44.0	43.7	43.7	43.2	44.2
MnO	2.17	2.24	1.75	2.63	2.49	0.82	0.73	0.81	1.84	1.98	1.69	2.40	2.11
MgO	0.12	0.25	0.08	0.03	0.05	0.11	0.11	0.22	0.02	--	0.03	0.03	--
CaO	0.13	0.13	0.13	0.13	0.13	0.22	0.21	0.23	0.09	0.06	0.04	0.05	0.08
Total	100.9	100.9	99.0	100.9	100.4	101.1	100.0	101.1	101.2	100.4	100.1	100.2	101.1
Mole % R_2O_3	5.7	5.8	4.8	3.1	3.5	0.8	2.3	1.6	4.0	3.7	4.1	3.7	3.0
≠T°C	<600	<600	590						680	650	710	710	680
-log f_{O_2}	<20	<20	20.3						18.2	19.0	17.5	17.5	18.8

Total iron was determined and the amounts of Fe_2O_3 and FeO were calculated using the method of Carmichael (1967).

≠Temperatures and oxygen fugacities were determined from the T-f_{O_2}-X data of Buddington and Lindsley (1964).

1, 2, 3 etc. Individual point analysis of ferrian ilmenite lamella and titaniferous magnetite host adjacent to the lamella. Sample numbers without superscripts are for points removed from lamellae.

--, not detected.

grains of the same specimen is less than 5 percent of the amount of the oxide present. Although there are some inconsistencies in the amounts of minor elements, the bulk analyses should at least approximate the average composition of the ilmeno-magnetite and hence approximate the composition of the titaniferous magnetite that formed by granule 'exsolution' of Stage II.

Fractionation trends of the oxide minerals

The compositional change with stratigraphic height of the cumulus pyroxenes (Himmelberg and Ford, 1976) and bulk rock mafic index [100 $(FeO+Fe_2O_3)/(FeO+Fe_2O_3+MgO)$] (Ford, 1970) is one of general enrichment in iron. Exceptions to this trend are: (1) a 1 km thick section in the lower part of the body that shows slight to no iron-enrichment, and (2) a marked reversal in the Fe/(Fe+Mg) ratio at about the 600–700 m level in the Forrestal Range section. These deviations from the general trend are associated with parts of the column showing an abundance of meter-scale, mineral-graded layers. Such layers are believed to be related to convection, and therefore the variations may be the result of

Table 3. Analyses of ilmeno-magnetite and ferrian ilmenite of composite grains of the Dufek intrusion

Ilmeno-Magnetite	266Fa	79Fa	74Fa	86Fa	310Fa	171Fa	161Fa	164Fa
TiO_2	11.1	15.0	15.0	13.7	13.4	14.6	11.2	18.8
Al_2O_3	2.29	1.70	1.53	1.59	2.24	1.91	1.40	0.80
V_2O_3	2.21	1.57	n.d.	0.50	1.28	0.82	0.11	0.15
*Fe_2O_3	41.9	37.9	37.9	40.8	38.8	36.9	44.7	30.0
FeO	40.5	44.7	44.2	43.4	42.9	43.7	40.6	47.6
MnO	0.30	0.30	0.65	0.34	0.42	0.26	0.48	0.75
MgO	0.36	0.58	0.13	0.33	0.22	0.34	0.10	0.02
Total	98.6	101.7	99.4	100.8	99.4	98.5	98.6	97.8
Mole % Ulvospinel	31.7	41.5	42.6	38.4	38.0	41.7	32.3	54.4

Ilmenite	266Fa	79Fa	74Fa	86Fa	310Fa	171Fa	161Fa
SiO_2	0.38	0.16	0.46	n.d.	0.29	0.41	0.49
TiO_2	50.6	50.0	49.4	50.3	50.6	50.3	52.0
Al_2O_3	0.19	0.19	0.12	0.05	0.12	0.14	0.09
Cr_2O_3	--	--	0.07	--	--	--	--
V_2O_3	0.44	0.56	n.d.	0.51	0.46	0.39	0.27
*Fe_2O_3	4.67	4.82	5.52	4.84	3.44	4.89	0.21
FeO	41.8	42.6	43.1	43.6	44.1	44.2	45.2
MnO	0.48	0.43	1.20	0.72	1.17	0.52	1.84
MgO	2.06	1.12	0.25	0.48	0.20	0.45	0.06
CaO	--	0.12	0.14	n.d.	0.16	0.19	0.13
Total	100.6	100.0	100.3	100.5	100.6	101.9	100.3
Mole % R_2O_3	5.1	5.4	5.5	5.2	3.9	5.2	0.6
≠T°C	730	790	790	760	730	790	
$-\log f_{O_2}$	16.6	15.2	15.1	15.8	17.1	15.2	

Total iron was determined and the amounts of Fe_2O_3 and FeO were calculated using the method of Carmichael (1967).

≠*Temperatures and oxygen fugacities were determined from the T-f_{O_2}-X data of Buddington and Lindsley (1964).*

--, *not detected; n.d., not determined.*

mixing of different batches of magma within a chamber.

Titanium and iron contents of the oxide minerals are largely controlled by subsolidus recrystallization, and thus do not show any regular variation with stratigraphic height that can be related to differentiation of the magma. However, weight percent V_2O_3 and Al_2O_3 in ilmeno-magnetite do show fractionation trends correlative with stratigraphic height (Fig. 4). The cation ration Mg/(Mg+Fe) of coexisting calcium-rich pyroxenes is plotted to illustrate the general fractionation trend of this part of the intrusion (Fig. 4).

Contents of both V_2O_3 and Al_2O_3 in ilmeno-magnetite decrease with fractionation, and show a sharp reversal at the same level that a reversal in Mg/(Mg+Fe) cation ratio occurs in the pyroxene trend. The results suggest that the distribution of V_2O_3 and Al_2O_3 has been little affected by subsolidus reequilibration. Because of strong partitioning of Al_2O_3 and V_2O_3 into the spinel phase, the titaniferous magnetite host should show the same variation with stratigraphic height as the ilmeno-magnetite. However, variations in titaniferous magnetite host compositions are easily obscured by perturbations resulting from including different amounts of ferrian ilmenite lamellae in individual analyses. This complexity is eliminated by using the bulk ilmeno-magnetite compositions. Similar variation of iron–titanium oxides

Table 4. Calculated composition of titaniferous magnetite* and analyses of discrete ferrian ilmenite of the Dufek intrusion

Magnetite	74Fa	171Fa
SiO_2	0.54	0.46
TiO_2	27.5	23.4
Al_2O_3	1.18	1.31
Cr_2O_3	0.38	0.03
Fe_2O_3	28.9	32.8
FeO	39.5	42.1
MnO	0.98	0.39
MgO	0.19	0.34
CaO	0.12	0.22
Total	99.3	101.0
Mole % Ulvospinel	64.4	57.9

Ilmenite	74Fa	171Fa
SiO_2	0.60	n.d.
TiO_2	49.3	50.0
Al_2O_3	0.21	--
Cr_2O_3	0.04	--
**Fe_2O_3	5.30	5.08
FeO	43.3	43.2
MnO	0.79	0.54
MgO	0.42	0.69
CaO	0.13	n.d.
Total	100.1	99.51
Mole % R_2O_3	5.4	4.9
≠T°C	960	890
$-\log f_{O_2}$	11.9	13.2

Composition of titaniferous magnetite calculated by combining the composition of titaniferous magnetite host, ferrian ilmenite lamellae, and ferrian ilmenite of composite grains in the proportions indicated by modal data.

**Total iron was determined and the amounts of Fe_2O_3 and FeO were calculated using the method of Carmichael (1967).*

≠*Temperatures and oxygen fugacities were determined from the T-f_{O_2}-X data of Buddington and Lindsley (1964).*

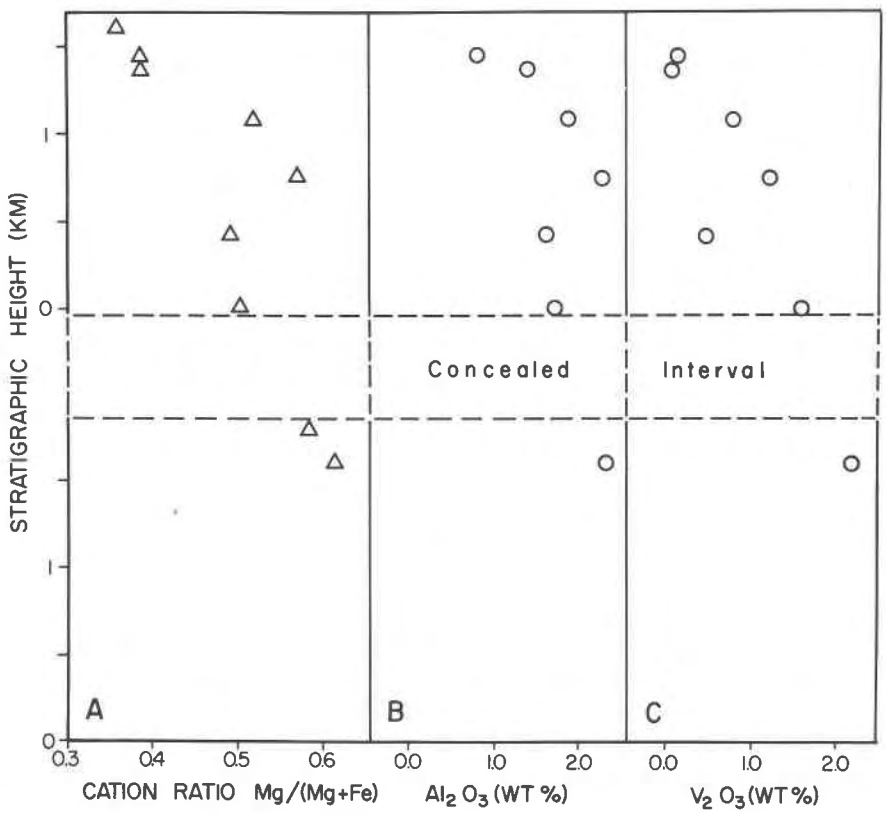

Fig. 4. Variation of mineral composition with stratigraphic height: (A) cation ratio Mg/(Mg+Fe) for calcium-rich pyroxene (Himmelberg and Ford, 1976); (B) weight percent Al_2O_3 in ilmeno-magnetite; and (C) weight percent V_2O_3 in ilmeno-magnetite.

with differentiation has been shown for the Skaergaard (Vincent and Phillips, 1954) and Somerset Dam intrusions (Mathison, 1975).

Crystallization conditions of the oxide minerals

Buddington and Lindsley's (1964) T-f(O2)-X relations can be used to determine the conditions of crystallization of 'magnetite'-'ilmenite' pairs, provided they crystallized in equilibrium with each other and retained their original compositions. Application of the Buddington and Lindsley data to 'magnetite'-'ilmenite' pairs from volcanic rocks has proved to be a reliable indicator of liquidus conditions (Buddington and Lindsley, 1964; Carmichael, 1967; Anderson, 1968). Iron-titanium oxides from plutonic rocks have invariably undergone subsolidus recrystallization, and do not provide data for directly determining conditions of primary magmatic crystallization (Buddington and Lindsley, 1964; Smith, 1970; Mathison, 1975); instead their compositions reflect complexities of subsolidus recrystallization, and primary conditions must be inferred.

The existing iron-titanium oxides in the Dufek intrusion are interpreted to be a result of a minimum of three stages of crystallization: Stage I—magmatic crystallization, Stage II—granule 'exsolution,' and Stage III—lamellae 'exsolution.' The manganese content of successive generations of ferrian ilmenite is consistent with the experimentally-determined distribution of MnO between magnetite and ilmenite with decreasing temperature, and suggests that each generation of ferrian ilmenite was closed and did not re-equilibrate during later stages (Lindsley, 1976, written communication). Thus the compositions of discrete ferrian ilmenite (Table 4), ferrian ilmenite of composite grains (Table 3), and ferrian ilmenite lamellae (Table 2) are assumed to be representative of Stage I, Stage II, and Stage III, respectively. To apply Buddington and Lindsley's (1964) T-f(O2)-X relations to determine the temperature and oxygen fugacity conditions of each stage of crystallization, the composition of titaniferous magnetite that coexisted with the ferrian ilmenite of each stage must be determined.

No primary titaniferous magnetite is preserved, but the composition of the titaniferous magnetite prior to any unmixing was calculated for two samples. Modal proportions of titaniferous magnetite

host, ferrian ilmenite lamellae, and ferrian ilmenite of composite grains were determined by point counting on all oxide mineral grains in each sample. The modal data, converted to weight percent, were combined with the average composition of each of the above iron–titanium oxide minerals to yield a composition approximating that of the titaniferous magnetite before the beginning of 'exsolution.' By this method values of 64.4 mole percent $TiFe_2O_4$ (sample 74Fa) and 57.9 mole percent $TiFe_2O_4$ (sample 171Fa) were obtained (Table 4). An alternate calculation using the compositions and modal proportions of ilmeno-magnetite and ferrian ilmenite of composite grains yielded similar values of 60.6 and 58.0 mole percent $TiFe_2O_4$ for these samples. The calculated compositions of titaniferous magnetite paired with the compositions of discrete ferrian ilmenite yield temperature and oxygen fugacity values of 960°C, $10^{-11.9}$ bar and 890°C, $10^{-13.2}$ bar.

These temperatures are obviously too low to represent conditions on the liquidus, and cannot be attributed to inaccuracies in the modal data. The composition of the primary titaniferous magnetite of sample 74Fa is estimated to have been about 77 mole percent $TiFe_2O_4$ (see below); and to obtain this value by recalculation would require a change in the modal proportions of titaniferous magnetite host and ferrian ilmenite of about 18 percent. Errors expected from point counting would only be about plus or minus 3 percent (Plas and Tobi, 1965). Furthermore, Mathison (1975), using a similar method, obtained equally low temperature values for 15 samples from the Somerset Dam intrusion. Mathison used a sufficient number of samples to expect that errors in temperature resulting from errors in modal data would be equally distributed about the liquidus temperature rather than yielding only temperature values lower than expected for the liquidus.

Consequently we conclude that for the Dufek intrusion, and possibly for other mafic intrusions as well, the primary magnetite composition cannot be obtained by recalculation methods. After magmatic crystallization and prior to any 'exsolution' the bulk composition of the titaniferous magnetite was apparently enriched in iron, possibly by reaction with the intercumulus liquid. The composition of the discrete ferrian ilmenite may also have been modified after magmatic crystallization, but it is believed that cooling of the Dufek intrusion was along ilmenite isopleths, so any change in major constituents of the discrete ferrian ilmenite was probably small.

Probably the best estimate of oxygen fugacity during magmatic crystallization is obtained for sample 74Fa by combining the composition of discrete ferrian ilmenite (Table 4) with the temperature of crystallization obtained from pyroxene geothermometry. Pyroxene compositions (Himmelberg and Ford, 1976) and temperature-composition relations in the system $CaSiO_3$–$MgSiO_3$–$FeSiO_3$ (Ross and Huebner, 1975) yield a temperature of cumulus pyroxene crystallization of approximately 1090°C. Assuming the cumulus iron–titanium oxides crystallized at the same temperature, the data applied to Buddington and Lindsley's (1964) experimental relations yield and oxygen fugacity of $10^{-10.1}$ bar at the time of crystallization of sample 74Fa. The original titaniferous magnetite composition is then inferred to have been approximately 77 mole percent $TiFe_2O_4$.

All samples except 164Fa have textures indicative of Stage II granule 'exsolution.' Compositions of Stage II titaniferous magnetite, as approximated by bulk analyses of ilmeno-magnetite, range from 31.7 to 42.6 mole percent $TiFe_2O_4$ (Table 3). These compositions paired with the compositions of coexisting ferrian ilmenite of composite grains (Table 3) yield temperature and oxygen fugacity values ranging from 790° to 730°C and $10^{-15.1}$ to $10^{-17.1}$ bar for the conditions of granule 'exsolution.'

Different ferrian ilmenite lamellae within the same host grain may have significantly different R_2O_3 contents, and titaniferous magnetite host is chemically inhomogeneous. Particularly, points adjacent to ferrian ilmenite lamellae are depleted in titanium and enriched in iron relative to points more removed from the lamellae. These data suggest that equilibrium during Stage III lamellae 'exsolution,' if obtained, was local, and is best represented by the compositions of adjacent ferrian ilmenite lamellae and titaniferous magnetite host (Table 2). One titaniferous magnetite host-ferrian ilmenite lamella pair from sample 74Fa yields a temperature of 590°C and and oxygen fugacity of $10^{-20.3}$ bar. Two other pairs from the same sample do not yield precise values, but indicate temperature and oxygen fugacity values less than 600°C and 10^{-20} bar. For sample 164Fa temperature and oxygen fugacity values range from 710° to 650°C and $10^{-17.5}$ to $10^{-19.0}$ bar. Although the data are few, they suggest that if the compositions of adjacent host and lamellae do represent equilibrium then lamellae 'exsolution' occurred over a range of temperature and oxygen fugacity values.

The temperature and oxygen fugacity values determined for crystallization, granule 'exsolution,' and lamellae 'exsolution' are plotted in Figure 5. Values for most samples fall near the conditions of the QFM (quartz–fayalite–magnetite) buffer. On the other

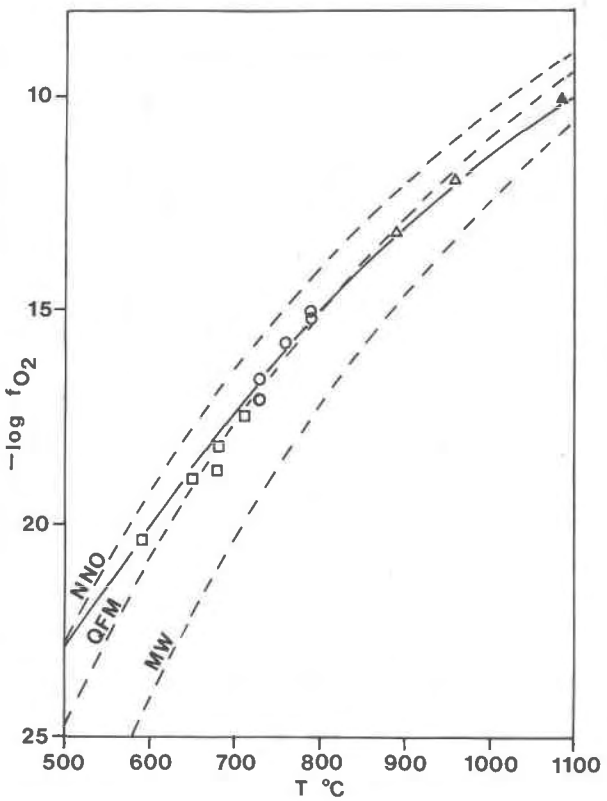

Fig. 5. T–$f(O_2)$ conditions indicated by the composition of iron–titanium oxide minerals of the Dufek intrusion. Square, titaniferous magnetite host–ferrian ilmenite lamella pair; circle, ilmeno-magnetite–ferrian ilmenite of composite grain pair; open triangle, reconstituted titaniferous magnetite–discrete ferrian ilmenite pair; closed triangle, oxygen fugacity inferred for Dufek magma using pyroxene geothermometry and composition of discrete ilmenite from sample 74Fa. Solid curve Hem_5Ilm_{95} isocompositional line from Buddington and Lindsley (1964). Positions of the NNO (nickel–nickel oxide), QFM (quartz–fayalite–magnetite), and MW (magnetitute–wüstite) buffers are from Eugster and Wones (1962), corrected for total pressure of 2000 bars.

hand, some ferrian ilmenite lamellae and ferrian ilmenite from composite grains from the upper 400 meters of the Dufek intrusion have lower R_2O_3 contents (0.1 to 2.8 percent, sample 161Fa Table 3 and unpublished analyses), and although precise temperature and oxygen fugacity values are indeterminate, many of the values would be close to the conditions of the MW (magnetite–wüstite) buffer.

For the two samples (74Fa and 171Fa) for which complete data are available, the manganese content of successive generations of ferrian ilmenite suggests that, once formed, the ferrian ilmenite was compositionally closed and did not reequilibrate during later stages (Lindsley, 1976, written communication). However, with the exception of some ferrian ilmenite lamellae, the R_2O_3 content of successive generations of ferrian ilmenite are similar. These data suggest that, at least for these two samples, cooling took place along temperature–oxygen fugacity trajectories essentially along ferrian ilmenite isopleths. If this model can be extrapolated to other samples, then most of the Dufek intrusion that crystallized cumulus oxide minerals cooled along trajectories close to the experimental Hem_5Ilm_{95} isopleth.

During crystallization and cooling of the Dufek intrusion the inferred oxygen fugacities were lower than those of the Somerset Dam intrusion, which plot near the NNO (nickel–nickel oxide) experimental buffer curve (Mathison, 1965), but were similar to those of the Skaergaard intrusion (Buddington and Lindsley, 1964). Possible factors causing the difference in oxygen fugacity during crystallization and cooling of the Dufek and Somerset Dam intrusions include the composition of the melt (Yoder and Tilley, 1962; Carmichael and Nicholls, 1967), the nature of the equilibria between the condensed phases (Nash and Wilkinson, 1970), and the amount of H_2O present (Hamilton and Anderson, 1967).

Conclusions

Although major-element contents of iron–titanium oxide minerals are affected by subsolidus crystallization, the amount of vanadium and aluminum in ilmeno-magnetite can be used as reliable indicators of the fractionation trend of the magma during crystallization. Estimates of temperature and oxygen fugacity conditions during crystallization and subsolidus reequilibration suggest that most of the intrusion with cumulus iron–titanium oxide minerals cooled along ferrian ilmenite isopleths near the conditions of the QFM buffer. An oxygen fugacity of $10^{-10.1}$ bar at 1090°C is inferred for the Dufek magma.

Acknowledgments

This research was supported by grant AG-238 from the Office of Polar Programs, NSF. The electron microprobe used for this study was purchased by the University of Missouri with the assistance of NSF grant GA-18445. The manuscript benefited from critical reviews by Gerald K. Czamanske, F.C.W. Dodge, Donald H. Lindsley, and W. P. Nash, We would also like to acknowledge Donald Lindsley for pointing out the significance of the manganese data and for suggesting we consider the implications of the data relative to cooling along ilmenite isopleths. However any errors in interpretation are the sole responsibility of the authors.

References

Anderson, A. T. (1968) The oxygen fugacity of alkaline basalt and related magmas, Tristan da Cunha. *Am. J. Sci., 266,* 704–727.

Behrendt, J. C., J. R. Henderson, L. Meister and W. L. Rambo

(1974) Geophysical investigations of the Pensacola Mountains and adjacent glacierized areas of Antarctica. *U.S. Geol. Survey Prof. Paper, 844.*

Buddington, A. F., J. Fahey and A. Vlisidis (1963) Degree of oxidation of Adirondack iron oxide and iron-titanium oxide minerals in relation to petrogeny. *J. Petrol., 4,* 138–169.

——— and D. H. Lindsley (1964) Iron-titanium oxide minerals and synthetic equivalents. *J. Petrol., 5,* 310–357.

——— and J. Nicholls (1967) Iron-titanium oxides and oxygen fugacities in volcanic rocks. *J. Geophys. Res., 72,* 4665–5687.

Czamanske, G. K. and P. Milhálik (1962) Oxidation during magmatic differentiation, Finnmarka Complex, Oslo area, Norway: Part 1, The opaque oxides. *J. Petrol., 13,* 493–509.

Eugster, H. P. and D. R. Wones (1962) Stability relations of the ferruginous biotite, annite. *J. Petrol., 3,* 82–125.

Ford, A. B. (1970) Development of the layered series and capping granophyre of the Dufek intrusion of Antarctica. In D.J.L. Visser and G. Von Gruenwaldt, Eds., *Symposium on the Bushveld Igneous Complex and Other Layered Intrusions,* p. 492–510. Geol. Soc. South Africa, Spec. Publ., 1.

——— (1976) Stratigraphy of the layered gabbroic Dufek intrusion of Antarctica. *U.S. Geol. Survey Bull. 1405-D, D1-D36.*

——— and W. W. Boyd, Jr. (1968) The Dufek intrusion, a major stratiform gabbroic body in the Pensacola Mountains, Antarctica. *23rd Int. Geol. Congr., 2,* 213–228.

Hamilton, D. L. and G. M. Anderson (1967) Effects of water and oxygen pressures on the crystallization of basaltic magmas. In H. H. Hess and A. Poldervaart, Eds., *Basalts, the Poldervaart Treatise on Rocks of Basaltic Composition,* p. 445–482. Interscience Publishers, New York, London, and Sydney.

Himmelberg, G. R. and A. B. Ford (1975) Petrologic studies of the Dufek intrusion Pensacola Mountains: Iron-titanium oxides. *Antarctic J. U.S., 10,* 241–243.

——— and A. B. Ford (1976) Pyroxenes of the Dufek intrusion, Antarctica. *J. Petrol., 17,* 219–243.

Mathison, C. I. (1975) Magnetites and ilmenites in the Somerset Dam layered basic intrusion, southeastern Queensland. *Lithos, 8,* 93–111.

Nash, W. P. and J. F. G. Wilkinson (1970) Shonkin Sag Laccolith, Montana I. Mafic minerals and estimates of temperature, pressure, oxygen fugacity, and silica activity. *Contrib. Mineral. Petrol., 25,* 241–269.

Neumann, E. (1974) The distribution of Mn^{2+} and Fe^{2+} between ilmenites and magnetites in igneous rocks. *Am. J. Sci., 274,* 1074–1088.

Plas, L. van der and A. C. Tobi (1965) A chart for judging the reliability of point counting results. *Am. J. Sci., 263,* 87–90.

Ross, M. and J. S. Huebner (1975) A pyroxene geothermometer based on composition-temperature relationships of naturally occurring orthopyroxene, pigeonite, and augite (abstr.). *International Conference on Geothermometry and Geobarometry,* The Pennsylvania State University, University Park, Pennsylvania.

Smith, Douglas (1970) Mineralogy and petrology of the diabasic rocks in a differentiated olivine diabase sill complex, Sierra Ancha, Arizona. *Contrib. Mineral. Petrol., 27,* 95–113.

Vincent, E. A. and R. Phillips (1954) Iron-titanium oxide minerals in layered gabbros of the Skaergaard intrusion East Greenland. Part I, Chemistry and ore-microscopy. *Geoch. Cosmoch. Acta, 6,* 1–26.

Yoder, H. S. and C. E. Tilley (1962) Origin of basalt magmas: An experimental study of natural and synthetic rock systems. *J. Petrol., 3,* 342–532.

Manuscript received September 16, 1976; accepted for publication, February 25, 1977.